MINERALOGICAL MAGAZINE

VOLUME 57 NUMBER 389 DECEMBER 1993

The origins of contrasting zoning patterns in hyalophane from olivine leucitites, Northeast China

MING ZHANG*

Department of Geology, Imperial College, London SW7 2BP, U.K., and Department of Geological Sciences, Southern Methodist University, Dallas, TX 75275, U.S.A.

PAUL SUDDABY

Department of Geology, Imperial College, London SW7 2BP, U.K.

ROBERT N. THOMPSON

Department of Geological Sciences, University of Durham, Durham DH1 3LE, U.K.

AND

MICHAEL A. DUNGAN

Department of Geological Sciences, Southern Methodist University, Dallas, TX 75275, U.S.A.

Abstract

Olivine (ol) leucitite lavas from Northeast China contain hyalophanes with contrasting Ba-zoning patterns. The hyalophanes occur: (1) in a magmatic inclusion (DZ2n), consisting of barian–titanian phlogopite + hyalophane + leucite + sodalite, and (2) as a mantle surrounding a sanidine megacryst (DZ19). Hyalophanes contain 4.6–20.2 mol.% celsian (Cn). The DZ2n hyalophane is normally zoned with respect to Ba (decreasing Ba toward rim), whereas the hyalophane mantle of megacryst DZ19 is reversely zoned. DZ2n probably crystallised from an extensively evolved (>80 wt.% crystallisation) potassic melt derived from a primitive magma chemically similar to the host, at relatively low temperatures and pressures (e.g. T~720 °C, P~2 kbar). Competition with barian–titanian phlogopite for Ba, and limited Ba supply from the residual melt are the main cause for the normal Ba zonation. Sanidine megacryst DZ19 originated as a high P–T product (e.g. T >950 °C, P >15 kbar) of an evolved leucite (lc) basanite/trachybasalt genetically related to ol-leucitites. Subsequently, it was incorporated into the host ol-leucititic magma at which point it was partially resorbed and then mantled by hyalophane. An increase in $K_{Ba}^{af/liq}$ values with decreasing temperature and pressure and co-crystallisation of the hyalophane mantle with Ba-free phases may have caused the unusual reverse zonation.

KEYWORDS: zoning, hyalophane, leucitites, China, olivine.

Introduction

HYALOPHANE (alkali feldspar with $BaAl_2Si_2O_8$ >5 mol.%, Deer *et al.*, 1963) is not uncommon in alkaline, particularly potassic, igneous rocks. Occurrences have been reported from: (1) ultra-potassic volcanic rocks (e.g. Nakamura and Yoder, 1973; Cundari, 1979; van Kooten, 1980; Ferguson and Cundari, 1982), (2) lamprophyres (e.g. Larsen, 1981; LeCheminant *et al.*, 1987;

* Present address: School of Earth Sciences, Macquarie University, NSW 2102, Australia.

Hamilton and Rock, 1990), (3) potassic intrusive rocks (e.g., Langworthy and Black, 1978; Flohr and Ross, 1990), and (4) some alkaline silicic lavas (e.g. Whitney *et al.*, 1988). These investigations suggest that hyalophane occurs mainly as a late-stage phase during crystallisation of evolved K-rich magmas and, in most cases, is normally zoned (i.e. decreasing Ba toward rim). In this paper we present new data for hyalophanes in ol-leucitites from Northeast China, with both normal and reverse zoning, and discuss their origins.

The ol-leucitites which host hyalophane are eruptive products of Dangzishan volcano, Keluo volcanic field, Northeast China (126°00′E, 48°00′N). The Keluo field, together with the neighbouring Wudalianchi and Erkeshan (WEK) fields (Zhang *et al.*, 1991) constitutes the Chinese potassic volcanic province. Three types of potassic volcanic rocks, ol-leucitite, lc-basanite and trachybasalt, are present. Ol-leucitites erupted during the late Miocene (9.6–7.0 Ma); whereas lc-basanites and trachybasalts are Pleistocene (0.56–0.13 Ma) and Recent (1719–1721 A.D.) (Zhang *et al.*, 1991).

Ol-leucitites (SiO_2 = 43–45 wt.%) contain olivine (8–13%), clinopyroxene (2–4%) and leucite (14–20%) microphenocrysts in a matrix of olivine, clinopyroxene, leucite, Fe-Ti oxides, nepheline, phlogopite and sodalite. Lc-basanites and trachybasalts (SiO_2 = 47–55 wt.%), on the other hand, have a phenocrystic assemblage of olivine (4–9%) ± clinopyroxene (0–11%) ± leucite (0–7%). Groundmass phases are predominantly K-feldspar (up to 50%) and clinopyroxene (up to 35%) plus subordinate leucite, olivine and Fe–Ti oxides. These WEK potassic rocks contain 3.6–7.1 wt.% K_2O and have K_2O/Na_2O >1. Ba contents are 1300–2200 ppm, without systematic variations in Ba among the three types of potassic rocks.

Occurrences of hyalophane

Hyalophanes occur in a magmatic inclusion (DZ2n) and as a mantle surrounding a sanidine megacryst (DZ-19) in Keluo ol-leucitites.

Inclusion DZ2n. DZ2n is a hypidiomorphic-textured tiny inclusion (<1 cm) hosted by an ol-leucitite (DZ-2-1). It is composed of barian–titanian phlogopite, hyalophane, leucite, and sodalite. Phlogopites are up to 0.3 mm in size and exhibit very strong, distinctive red-brown to pinkish-yellow pleochroism. Hyalophanes vary from 1.5 to 0.2 mm in size. Leucites are about 0.1–0.2 mm in size and weakly anisotropic. Isotropic sodalites occur as euhedral hexagonal grains (0.10–0.15 mm).

Petrographic evidence for the relationship between DZ2n and host magma is ambiguous. Neither a chilled margin nor a graduation in grain size has been observed adjacent to the host-inclusion boundary. This implies that either the inclusion was entrained in the host when it was not completely consolidated or it crystallised slowly in a vesicle from the cooling host melt.

Sanidine megacryst. Alkali feldspar megacrysts (Or_{49-69}) occur as ellipsoid-shaped crystals, up to 20 mm. X-ray diffraction (Qiu *et al.*, 1989) reveals that they are monoclinic and highly disordered ($T_1(0)$ = 0.26–0.27) sanidine. Fig. 1 is a back-scattered image of megacryst DZ-19. It is 8.6 mm in diameter and surrounded by a hyalophane mantle about 0.8 mm wide. Glassy inclusions with high Si and Al, but low analytical totals, occur in the mantle, together with leucite and oxides. The transition between the core and the mantle is sharp, but the sanidine apparently underwent corrosion prior to formation of the hyalophane overgrowth (Fig. 1).

Feldspar chemistry

All the mineral phases in inclusion DZ2n and sanidine megacryst DZ-19 have been analysed for

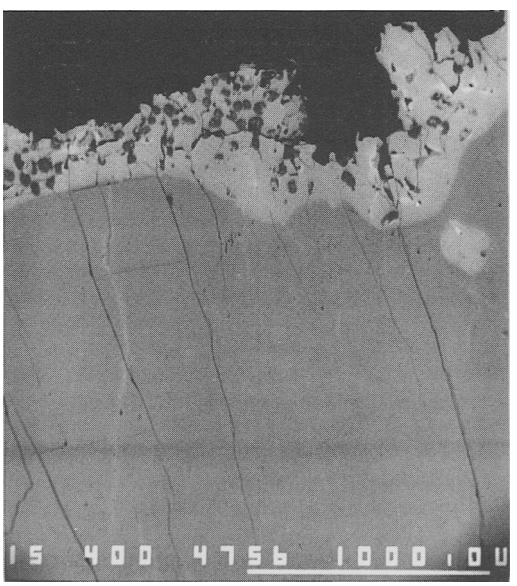

FIG. 1. Back-scattered image of megacryst DZ-19 showing a sanidine core (dark) mantled by hyalophane (bright). Tiny inclusions in the mantle are leucite, Fe–Ti oxides, and glass.

this study. Representative results are listed in Tables 1 and 2 respectively. Barian–titanian phlogopite in DZ2n is discussed in another paper (Zhang *et al.*, 1993).

Inclusion DZ2n. Hyalophanes from DZ2n are heterogeneous in K_2O, Na_2O, and BaO contents. Their Or and Ab mol.% range 57.0–44.7 and 31.2–40.2 respectively. BaO varies from 2.5 to 10.6%, equivalent to 4.6–20.2 mol.% of celsian (Cn). CaO contents are low (0.02–0.28 wt.%), with most samples having <0.7 mol.% of An. SrO contents are moderate (0.54–0.93 wt.%), equivalent to 1.6–2.6 mol.% of slawsonite (Sl). Therefore, the hyalophanes can be represented approximately in the Or–Ab–Cn ternary system (Fig. 2*a*). Iron contents (as Fe_2O_3) vary between 0.71 and 1.10 wt.%, similar to those in coexisting leucite and sodalite (Table 1).

DZ2n hyalophanes exhibit Ba variations among and within individual crystals. In general, the larger the grain size, the higher the BaO content. For instance, the crystals of 1.5, 0.8 and 0.2 mm in the elongated dimension have Cn of 20.2, 9.6 and 8.6 mol.% in their cores respectively. In accordance with this trend, the hyalophane grains display normal zoning. Two analytical traverses show that Cn decreases outward from 20.2 to 8.9 and from 16.2 to 4.6 respectively,

Table 1. Representative analyses of mineral phases in inclusion DZ2n

Ana. No.	1	2	3	4	5	6	7
SiO_2	57.02	61.91	60.50	62.26	54.78	40.02	31.74
TiO_2	n.a.	n.a.	n.a.	n.a.	n.a.	n.a.	12.79
Al_2O_3	20.88	19.42	19.98	19.34	22.48	30.75	13.69
Fe_2O_3	1.10	0.99	0.96	0.96	1.05	0.81 (FeO)	9.81
CaO	0.13	0.18	0.07	0.08	0.16	0.14	0.10
SrO	n.a.	n.a.	0.87	0.87	n.a.	n.a. (MgO)	11.99
BaO	10.55	3.86	5.13	2.47	n.d.	n.d.	10.34
Na_2O	3.64	3.69	4.13	4.01	0.39	24.02	0.92
K_2O	7.18	9.50	8.10	9.15	20.56	0.27	5.47
Cl	n.a.	n.a.	n.a.	n.a.	n.a.	6.46	n.a.
Sum	100.50	99.55	99.74	99.14	99.42	101.01*	96.85
Or	44.7	57.8	49.4	55.6			
Ab	34.5	34.1	38.3	37.0			
Cn	20.2	7.2	9.6	4.6			
An	0.7	0.9	0.4	0.4			
Sl			2.4	2.4			
K/K+Na					0.970	0.0077	0.794

Note: 1-4, hyalophane; 5, leucite; 6, sodalite; 7, barian-titanian phlogopite. *, less O≡Cl.
n.d., not detected; n.a., not analysed.

Table 2. Representative analyses of sanidine megacryst DZ-19

Ana. No.	1	2	3	4
SiO_2	60.34	62.50	61.53	65.11
Al_2O_3	20.18	19.51	19.62	19.17
Fe_2O_3	0.84	0.74	0.78	0.22
CaO	0.04	0.13	0.05	0.17
BaO	6.43	3.60	4.97	0.25
Na_2O	3.96	3.96	3.71	4.25
K_2O	8.73	9.48	9.38	10.41
Sum	100.56	99.92	100.04	99.58
Or	52.1	56.7	56.6	60.9
Ab	35.9	36.0	34.0	37.8
Ce	11.8	6.6	9.2	0.5
An	0.2	0.7	0.2	0.8

Note: 1-4, megacryst DZ-19 (1-3, hyalophane mantle; 4, sanidine core). Microprobe analyses were performed at IC and SMU, using a Cambridge Instruments Microscan 5 electron microscope, fitted with a Link energy dispersive detector, and a JEOL 733 Superprobe, equipped with four wavelength dispersive detectors, respectively. In-house standards of benitoite ($BaTiSi_3O_9$) and synthetic $BaTiO_3$ were used to control the quality of Ba analysis.

whereas Or increases from 44.7 to 56.6 and from 46.4 to 57.0. Ab correlates negatively with Or. One of the traverses is illustrated in Fig. 3*a*.

Megacryst DZ-19. The core of sanidine megacryst DZ19 varies in composition between $An_{0.8}Ab_{31.1}Or_{67.1}Cn_{1.0}$ and $An_{0.9}Ab_{44.0}Or_{54.4}Cn_{0.7}$ (Table 2). It is continuously zoned with decreasing Or and increasing Ab outward (Fig. 3*b*). In terms of K/(K + Na) ratios, DZ-19 core is similar to the most K-rich groundmass feldspars from WEK lc-basanites and trachybasalts (Fig. 2*b*). CaO contents are low (0.09–0.25 wt.%). BaO contents (0.25–0.60 wt.%) are broadly similar to those anorthoclase megacrysts from alkalic basalts reported eleswhere (e.g., 0.01–0.55 wt.%, Guo *et al.*, 1992). Fe_2O_3 (0.02–0.47 wt.%) is lower than for the hyalophane mantle (0.47–1.10 wt.%), but comparable to the anorthoclase megacrysts studied by Irving and Frey (1984) and Mason *et al.* (1982) (0.10–0.31 wt.%).

The hyalophane mantle of megacryst DZ-19 has a compositional range of $Or_{58.6-52.0}Ab_{41.1-30.6}An_{0.1-1.2}Cn_{4.7-11.8}$, which is comparable to DZ2n hyalophanes, except that the highest BaO content (6.4 wt.%) is considerably lower than that of the latter (10.6 wt.%). BaO increases sharply from <0.5 wt.% to 2.5 wt.% within <20 μm distances across the core–mantle boundary. The hyalophane mantle is reverse-zoned in Ba (Cn increasing from 4.7 to 11.8 mol.% outward, Fig. 3*b*), whereas zoning patterns of Or and Ab are asymmetric. On one side of the crystal, Or decreases outward, but Ab exhibits an oscillatory variation. On the other side, the opposite occurs (Fig. 3*b*).

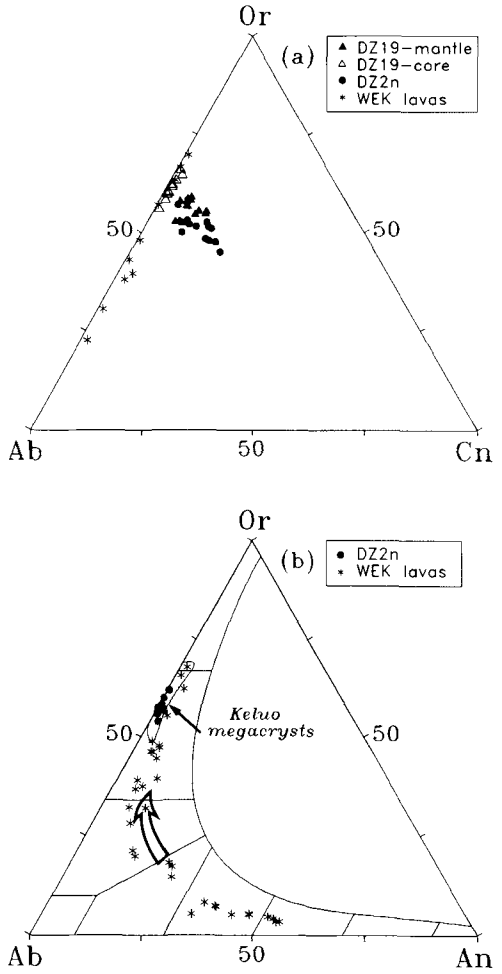

FIG. 2. Feldspar compositions from inclusion DZ2n, sanidine megacrysts, and the groundmass of WEK lc-basanites and trachybasalts. (*a*) Or–Ab–Cn system and (*b*) Or–Ab–An system. The groundmass plagioclase and ternary feldspars are omitted from Fig. 2(*a*). The arrow in Fig. 2(*b*) shows evolving trend of the groundmass feldspars. Data for some Keluo sanidine megacrysts from Qiu *et al.* (1989) are also included in Fig. 2(*b*).

Origins of hyalophanes and their contrasting zoning patterns

Most hyalophanes of magmatic origin are normally zoned and occur as a late interstitial phase in differentiates of alkaline mafic rocks. Flohr and Ross (1990) report K-feldspar rimmed by hyalophane mantle with a sharp contact in a garnet–nepheline syenite from Arkansas, USA. However, this hyalophane mantle is different from DZ-19 mantle in that its Ba content decreases as the outermost rim is approached. Therefore, the contrasting BaO zoning patterns displayed by the Keluo hyalophanes (Fig. 3) are unique and their origins warrant further explanation.

Hyalophane zoning patterns are apparently controlled by distribution coefficients for Ba between hyalophane and melt ($K_{Ba}^{af/liq}$) and by Ba contents of melts. The former is a function of pressure, temperature, melt composition, and possibly volatile contents (e.g. Guo and Green, 1989), whereas the latter depends on, among other factors, source characteristics, partial melting conditions, evolution pathways of parental magmas, and paragenesis. Although the lack of systematic experimental determination of K_d values precludes quantitative modelling, available data (e.g. Guo and Green, 1989; Long, 1978) provide qualitative constraints. These results collectively demonstrate that $K_{Ba}^{af/liq}$ is generally >1 and will increase with decreasing temperature and pressure, and increasing K_2O content in melt.

Inclusion DZ2n. Barian–titanian phlogopites from DZ2n have the same composition and substitution schemes as the groundmass phlogopites of ol-leucitites (Zhang *et al.*, 1993). DZ2n also has a mineral assemblage similar to that in the matrices of ol-leucitites, although hyalophane has not been found in the lavas. These resemblances led to Zhang *et al.*'s (1993) conclusion that DZ2n was generated from an extensively fractionated potassic melt derived from a primitive magma chemically similar to the Keluo ol-leucitites. They also suggest that the residual melt was highly enriched in volatile components, particularly in F and Cl, and crystallised at pressures higher (e.g. ~2 kbar) and temperatures lower (e.g. ~720 °C) than those for the matrix phases of ol-leucitites (near-surface pressure and ~960 °C respectively).

Both barian–titanian phlogopite and hyalophane are Ba repositories in DZ2n. Phlogopite contains higher BaO (11.3–8.4 wt.%) than hyalophane (10.6–2.5 wt.%), implying that $K_{Ba}^{phl/liq} > K_{Ba}^{af/liq}$. Similarly, distribution coefficients based on measured Ba abundances of phenocrysts and glassy matrix in alkalic mafic lavas and their derivatives suggest that, wherever both phases coexist as phenocrysts, the mica always has higher K_d values than the alkali feldspar (e.g. Villemant *et al.*, 1981; Wörner *et al.*, 1983; Francalanci *et al.*, 1987). Assuming the K_d of 11 for phlogopite (Villemant *et al.*, 1981; Wörner *et al.*, 1983) and of 9 for alkali feldspar (Guo and Green, 1989), the melt should contain about 1.1 wt.% BaO for crystallisation of barian–titanian phlogopite and

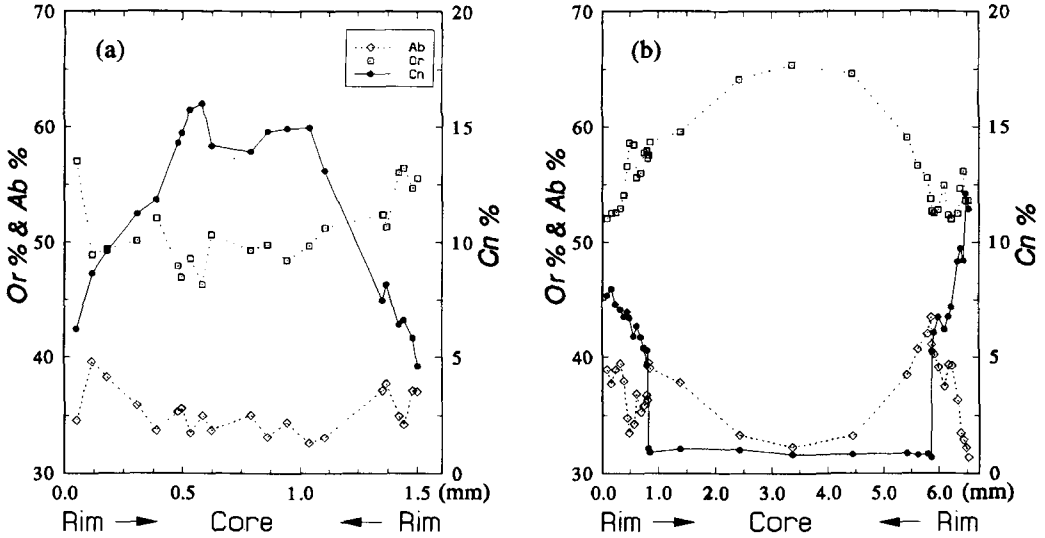

FIG. 3. Analytical traverses of (*a*) DZ2n hyalophane and (*b*) sanidine megacryst DZ-19.

hyalophane from DZ2n. As a silicate melt with about 1.2 wt.% BaO may still obey Henry's law (Guo and Green, 1989), Rayleigh fractionation is applicable. Keluo ol-leucitites contain about 0.2 wt.% of BaO. If this value approximates Ba-content in the parental magma for DZ2n and if Ba is considered completely incompatible for olivine, clinopyroxene, leucite, and Fe-Ti oxides, which is almost the case for Keluo ol-leucitites, at least 83% crystallisation of these phases is needed to enhance Ba-concentrations in the residual melt to such a level (>1 wt.%) as is necessary to form the barian–titanian phlogopite and hyalophane.

The Ba-rich cores of feldspars in DZ2n are consistent with precipitation at relatively low pressures and low magmatic temperatures, conditions under which Ba is strongly partitioned into the feldspar. Progressive Ba depletion of the residual melt, leading to normal zoning, is predictable because two Ba-rich phases, hyalophane and mica were co-precipitating. The absence of any zoning in the coexisting barian–titanian phlogopite is difficult to explain in conjunction with this model.

Sanidine megacryst DZ-19. Alkali feldspar megacrysts are common in alkalic basaltic rocks and some alkalic lamprophyres such as camptonites and monchiquites. Based on petrographic evidence, phase equilibrium experiments, and trace element and radiogenic isotopic data, it has been generally accepted that alkali feldspar megacrysts are not high-pressure phenocrysts of their hosts (e.g. Stuckless and Irving, 1976; Bahat, 1979; Irving and Frey, 1984). Instead, it is thought that they crystallized from benmoreitic (Guo *et al.*, 1992) or phonolitic (Aspen *et al.*, 1990) magmas at moderate or high pressures and subsequently were entrained by more primitive basaltic hosts during ascent at high temperatures.

Although we agree in general with the concept that alkali feldspar megacrysts are generated from evolved melts, and thus have never been in equilibrium with their host magmas, we want to address a broadly genetic relationship between megacrysts and hosts reflected by correlations in major element compositions between them. Fig. 4 shows the compositions of feldspar megacrysts from Keluo and other locations compiled from the literature. They are predominantly anorthoclase with subordinate sanidine and albitic plagioclase. Sanidine megacrysts are reported only from Prezazzo–Monzoni area, Italy (Lucchini *et al.*, 1969); Ubekendt Ejiand, Greenland (Larsen, 1981); Keluo, NE China (this work), and Scotland (Aspen *et al.*, 1990). The hosts for all the sanidine megacrysts except those from Scotland, whose compositions are not documented, are potassic (K_2O/Na_2O >1.0) mafic rocks. Alkali feldspar megacrysts are widespread in Cenozoic alkalic basalts from East China (Qui and Liu, 1987). There is a regional variation from North to South in the composition of these megacrysts, from sanidine through anorthoclase to potassic oligoclase (Fig. 4). This corresponds to a major element trend for the Chinese alkalic basalts; i.e. alkaline contents and K_2O/Na_2O decrease, and

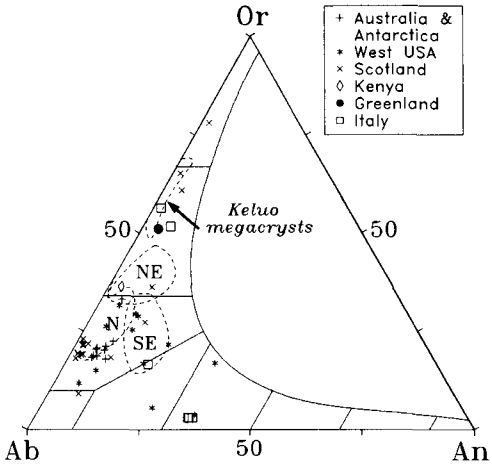

FIG. 4. Or–Ab–An ternary system for alkali feldspar megacrysts from Keluo and other locations. Areas labelled as NE, N and SE show compositions of Chinese alkali feldspar megacrysts from Northeast, North, and Southeast China respectively (Qiu and Liu, 1987). Other data sources: Lucchini *et al.* (1969); Hoffer and Hoffer (1973); Irving (1974); Laughlin *et al.* (1974); Bahat (1979); Mason *et al.* (1982); Irving and Frey (1984); Aspen *et al.* (1990). For the sake of clarity, 50% data points for megacrysts from Australia, West USA and Scotland are not plotted.

CaO increase from North to South (Chi, 1988). These co-variations imply a genetic connection between the megacryst-forming magmas and the megacryst-bearing magmas. The former may be derivatives of primative mafic magmas very similar to host magmas which have entrained the megacrysts. In a broad sense, these megacrysts cannot be regarded as entirely accidental xenocrysts. In particular, we conclude that the Keluo sandine megacrysts crystallised from evolved potassic magmas, which were temporally, spatially, and genetically associated with WEK potassic magmatism, but failed to reach the surface.

As olivine- and clinopyroxene-dominated fractionation cannot significantly increase SiO_2 content in a low-SiO_2 ol-leucititic magma, late-matrix phases in ol-leucitites include leucite, nepheline, sodalite, and phlogopite, without feldspar. In contrast, alkali feldspar is abundant in the matrices of lc-basanites and trachybasalts because fractionation of the same phases from a less SiO_2-undersaturated magma drives the residual liquids toward SiO_2-saturation. Consequently, the parental magma for megacryst DZ19 may have been an evolved WEK lc-basanite/trachybasalt, but not an ol-leucitite. The similarity in composition between the sanidine megacrysts and the late groundmass feldspar in lc-basanites and trachybasalts (Fig. 2*b*) supports this conclusion.

If BaO content of the parental magma for the Keluo megacrysts is similar to those of WEK lc-basanites and trachybasalts (0.15–0.22 wt.%), the low BaO contents (<0.60 wt.%) of the megacrysts require a $K_{Ba}^{af/liq}$ of about 3, indicating that they may have formed at $P \geq 15$ kbar and $T \geq 950$ °C (Guo and Green, 1989). Alternatively, if the evolved magma was *depleted* in Ba as a consequence of alkali feldspar crystallisation in the matrix, higher K_d and thus lower *P–T* environments are possible.

As alkali feldspar is not present as a groundmass phase in Keluo ol-leucitites, and the sanidine megacrysts underwent partial resorption prior to precipitation of the hyalophane mantle, we conclude that hyalophane would not have formed without the existence of the disequilibrium megacryst. These observations may be reconciled if melting of the sanidine enriched a boundary layer surrounding the megacryst in SiO_2, and the megacryst served as a nucleation site for the hyalophane mantle. Depending on the proportions of crystallising Ba-free phases and the partitioning of Ba in hyalophane, Ba may have been progressively enriched in the residual liquid during growth of the vanishingly small proportion of hyalophane. Moreover, $K_{Ba}^{af/liq}$ should increase with decreasing pressure and temperature. Whereas the residual liquid reservoir in the melt pocket from which inclusion DZ2n grew may have been small relative to the volume of hyalophane, the opposite was certainly true for the hyalophane mantling sanidine. These circumstances are sufficient to account for growth of the reversely zoned hyalophane from evolved potassic melts, as has been theoretically demonstrated for alkalic silicic melts by Long and Luth (1986).

In conclusion, we suggest that both normal and reverse zoning patterns in hyalophanes can be products of crystallisation from evolved potassic magmas, depending on the nature of coexisting phases, degree of crystallisation, and changes in intensive variables of the melts which, in turn, control K_d values. Competition with barian–titanian phlogopite for Ba and limited Ba supply from a residual melt are the main causes for normal Ba zoning in DZ2n hyalophane. On the other hand, increase in K_d values with decreasing temperature and pressure as well as increase in Ba content in the melt by concurrent crystallisation of Ba-free phases may have played an important role in the formation of the unusual reverse zoning in DZ19 hyalophane mantle.

Acknowledgements

Financial support for this study was provided by the late Stephen Hui through the Anna and Stephen Hui Fellowship at Imperial College, London, in Britain and by the Department of Geological Sciences at Southern Methodist University (SMU) in the USA to M. Z., and by a NSF grant EAR 90-04812 to M. A. D. We thank Mr. N. Royall, Mr. R. Giddens, and Mr. D. Deuring for their assistance in microprobe analysis. Two anonymous reviewers' constructive review substantially improved the manuscript.

References

Aspen, P., Upton, B. G. J., and Dickin, A. P. (1990) Anorthoclase, sanidine, and associated megacrysts in Scottish alkali basalts: high-pressure syenitic debris from upper mantle sources? *Eur. J. Mineral.*, **2**, 503–17.

Bahat, D. (1979) Anorthoclase megacrysts: physical conditions of formation. *Mineral. Mag.*, **43**, 287–91.

Chi, J. S. (1988) *The Study of Cenozoic basalts and upper mantle beneath Eastern China,* China Univ. Geosci, Press, Wuhan, China (in Chinese with English abstract).

Cundari, A. (1979) Petrogenesis of leucite-bearing lavas in the Roman volcanic region, Italy. *Contrib. Mineral. Petrol.*, **70**, 9–21.

Deer, W. A., Howie, R. A., and Zussman, J. (1963) *Rock-forming minerals, vol. 4. Framework silicates.* Longmans, London. 435 pp.

Ferguson, A. K. and Cundari, A. (1982) Feldspar crystallization trends in leucite-bearing and related assemblages. *Contrib. Mineral. Petrol.*, **81**, 212–8.

Flohr, M. J. and Ross, M. (1990) Alkaline igneous rocks of Magnet Cove, Arkansas: Mineralogy and geochemistry of syenites. *Lithos,* **26**, 67–98.

Francalanci, L., Peccerillo, A., and Poli, G. (1987) Partition coefficients for minerals in potassium-alkaline rocks: data from Roman Province (Central Italy). *Geochem. J.*, **21**, 1–10.

Guo, J. and Green, T. H. (1989) Barium partitioning between alkali feldspar and silicate liquid at high pressure and temperature. *Contrib. Mineral. Petrol.*, **102**, 328–35.

—— —— and O'Reilly, S. Y. (1992) Ba partitioning and the origin of anorthoclase megacrysts in basaltic rocks. *Mineral. Mag.*, **56**, 101–7.

Hamilton, R. and Rock, N. M. S. (1990) Geochemistry, mineralogy and petrology of a new find of ultramafic lamprophyres from Bulljah Pool, Nabberu Basin, Yilgarn Craton, Western Australia. *Lithos,* **24**, 275–90.

Hoffer, J. M. and Hoffer, R. L. (1973) Composition and structural state of feldspar inclusions from alkali olivine basalt, Potrillo basalt, southern New Mexico. *Geol. Soc. Amer. Bull.*, **84**, 2139–42.

Irving, A. J. (1974) Megacrysts from the Newer Basalts and other basaltic rocks of southeastern Australia. Ibid. **85**, 1503–14.

—— and Frey, F. A. (1984) Trace element abundances in megacrysts and their host basalts: Constraints on partition coefficients and megacryst genesis. *Geochim. Cosmochim. Acta,* **48**, 1201–21.

Langworthy, A. P. and Black, L. P. (1978) The Mordor Complex: a highly differentiated potassic intrusion with kimberlitic affinities in Central Australia. *Contrib. Mineral. Petrol.*, **67**, 51–62.

Larsen, J. G. (1981) Medium pressure crystallization of a monchiquitic magma—evidence from megacrysts of Drever's block, Ubekendt Ejland, West Greenland. *Lithos,* **14**, 241–62.

Laughlin, A. W., Manzer, G. K. Jr., and Carden, J. R. (1974) Feldspar megacrysts in alkali basalts. *Geol. Soc. Amer. Bull.*, **85**, 413–6.

LeCheminant, A. N., Miller, A. R., and LeCheminant, G. M. (1987) Early Proterozoic alkaline igneous rocks, District of Keewatin, Canada: petrogenesis and mineralization. In *Geochemistry and mineralization of Proterozoic volcanic rocks* (T. C. Pharaoh, R. D. Beckinsale, and D. Rickard, ed.), *Geol. Soc. London Spec. Publ.,* **33**, 219–40.

Long, P. E. (1978) Experimental determination of partition coefficients for Rb, Sr, and Ba between alkali feldspar and silicate liquid. *Geochim. Cosmochim. Acta,* **42**, 833–46.

—— and Luth, W. C. (1986) Origin of K-feldspar megacrysts in granitic rocks: Implications of a partitioning model for barium. *Am. Mineral.*, **71**, 367–75.

Lucchini, F., Mezzetti, R., and Simboli, G. (1969) The lamprophyres of the area Predazzo-Monzoni: Camptonites. *Miner. Petrogr. Acta,* **15**, 109–45.

Mason, R. A., Smith, J. V., Dawson, J. B., and Treves, S. B. (1982) A reconnaissance of trace elements in anorthoclase megacrysts. *Mineral. Mag.*, **46**, 7–11.

Nakamura, Y. and Yoder, H. S. Jr. (1973) Analcite, hyalophane, and phillipsite from the Highwood Mountains, Montana. *Carnegie Inst. Wash. Yearbook,* **72**, 354–8.

Qiu, J. X. and Liu, M. H. (1987) The characteristics and origin of feldspar megacrysts in Cenozoic basalts from some locations of east China. *Acta Mineralogica Sinica,* **7**, 37–46 (in Chinese with English abstract).

—— —— and Du, X. R. (1989) Pyroxene and feldspar megacrysts of K-rich volcanics from Keluo-Erkeshan, Heilongjiang province (NE China). *Scientia Geologica Sinica,* (**4**), 355–68 (in Chinese with English abstract).

Stuckless, J. S. and Irving, A. J. (1976) Strontium isotope geochemistry of megacrysts and host basalts from southereastern Australia. *Geochim. Cosmochim. Acta,* **40**, 209–13.

van Kooten, G. (1980) Mineralogy, petrology, and geochemistry of an ultrapotassic basaltic suite, central Sierra Nevada, California, U.S.A. *J. Petrol.*, **21**, 651–84.

Villemant, B., Jaffrezic, H., Joron, J. L., and Treuil, M. (1981) Distribution coefficients of major and trace elements; fractional crystallization in the alkali basalt series of Chaine des Puys (Massif Central, France). *Geochim. Cosmochim. Acta,* **45**, 1997–2016.

Whitney, J. A., Dorais, M. J., Stormer, J. C. Jr. Kline, S. W., and Matty, D. J. (1988) Magmatic conditions and development of chemical zonation in the Car-

penter Ridge tuff, Central San Juan volcanic field, Colorado. *Amer. J. Sci.* **288**, 16–44.

Wörner, G., Beusen, J-M., Duchateau, N., Gijbels, R., and Schmincke, H-U. (1983) Trace element abundances and mineral/melt distribution coefficients in phonolites from the Laacher See Volcano (Germany). *Contrib. Mineral. Petrol.*, **84**, 152–73.

Zhang, M., Menzies, M. A., Suddaby, P., and Thirlwall, M. F. (1991) EM1 signature from within the post-Archaean subcontinental lithospheric mantle: isotopic evidence from the potassic volcanic rocks in NE China. *Geochem. J.*, **25**, 329–340.

—— Suddaby, P., Thompson, R. N., and Dungan, M. A. (1993) Barian–titanian phlogopites from potassic lavas in northeastern China: Substitutions and paragenesis. *Am. Mineral.*, **78**, 1054–63.

[*Manuscript received 25 August 1992: revised 18 November 1992*]